ISSN 1063-7842, Technical Physics, 2019, Vol. 64, No. 1, pp. 121–126. © Pleiades Publishing, Ltd., 2019.
Russian Text © V.K. Krut'ko, V.V. Kazbanov, O.N. Musskaya, A.A. Gaidash, A.I. Kulak, N.M. Chekan, M.S. Serdobintsev, K.V. Skrotskaya, 2019, published in Zhurnal Tekhnicheskoi Fiziki, 2019, Vol. 89, No. 1, pp. 147–152.

BIOMEDICAL PHYSICS

Physicochemical Properties and Structure of the Bone Matrix in Simulated Tuberculous Osteitis

V. K. Krut'ko[a], V. V. Kazbanov[b,c], O. N. Musskaya[a,*], A. A. Gaidash[b,c], A. I. Kulak[a], N. M. Chekan[d], M. S. Serdobintsev[b], and K. V. Skrotskaya[e]

[a] *Institute of General and Inorganic Chemistry, National Academy of Sciences of Belarus, Minsk, 220079 Belarus*
[b] *St. Petersburg Research Institute of Phthisiopulmonology, St. Petersburg, 191036 Russia*
[c] *Republican Scientific and Practical Center for Pediatric Surgery, Minsk, 220013 Belarus*
[d] *Physicotechnical Institute, National Academy of Sciences of Belarus, Minsk, 220141 Belarus*
[e] *Research Institute of Physical and Chemical Problems, Minsk, 220030 Belarus*
**e-mail: tsuber@igic.bas-net.by*

Received March 26, 2018

Abstract—The physicochemical properties and structure of the bone matrix are studied in a case of simulated tuberculous osteitis without treatment and after a full course of specific antibacterial therapy. Using X-ray diffraction, infrared spectroscopy, thermal analysis, and scanning electron microscopy, we revealed that tuberculous osteitis causes fine disintegration of the bone matrix due to an increase in nonstoichiometric hydroxyapatite, formation of amorphous calcium phosphates, and a decrease of the organic phase, which is accompanied by embrittlement of the bone matrix. Excessive growth of carbonate-hydroxyapatite crystals of a mixed AB substitution type leads to excessive osteogenesis, accompanied by the uncontrolled growth of bone trabeculae. The presence of "liming" regions in the crystal lattice of hydroxyapatite increases the "binding" properties of the bone matrix in which mycobacteria are immobilized and removed in the composition of detritus.

DOI: 10.1134/S1063784219010183

INTRODUCTION

Tuberculous lesions of bones and joints are often found in clinical forms of extrapulmonary tuberculosis, which is difficult to diagnose and treat [1]. One of the earliest manifestations of developing tuberculous osteitis is osteoporotic transformation [2], which is complicated by focal disintegration and sequestration of the bone matrix. The mechanisms of osteoporotic transformation of the bone matrix and shifts in the processes of bone tissue remodeling in tuberculous osteitis remain mostly unclear. This is especially true for small forms, for example, vaccine osteitis, which are well amenable to specific antibacterial treatment and are prone to "self-healing." Under such conditions, osteoporosis is a trigger [2] creating structural and physicochemical prerequisites that lead to osteolysis and osteogenesis.

To date, the physicochemical properties of the mineral phase, regenerating bone, remain little studied, despite the fact that it is based on calcium phosphates constituting approximately 50% of the bone matrix volume, which largely determines the mechanical and structure-forming properties of the bone as a whole. Even less studied are the physicochemical transformations of the bone matrix in tuberculous osteitis, the incidence of which, especially in small forms, is increasing. The ultrastructural changes of the extracellular matrix during physiological remodeling of bone tissue are also not evident. The purpose of this paper was to study the physicochemical properties and ultrastructural changes of the bone matrix in normal conditions and under simulated tuberculous osteitis without treatment and after a full course of specific antibacterial therapy.

SAMPLES AND METHODS OF RESEARCH

The experiments were performed on mature male Chinchilla rabbits in the experimental laboratory of the Research Institute of Phthisiopulmonology (St. Petersburg). The protocols of experiments agree with the ethical committee and comply with the rules for working with laboratory animals, approved by the Ministry of Health of the Russian Federation. Control group 1 was composed of healthy rabbits. In rabbits of groups 2 and 3, tuberculous osteitis was simulated by introducing a culture of Mycobacterium tuberculosis into the meta-epiphysis of the femoral bones. After the formation of the primary focus (its presence was verified radiographically), necrotic masses were removed and observed for 1–2 months. Animals of group 2

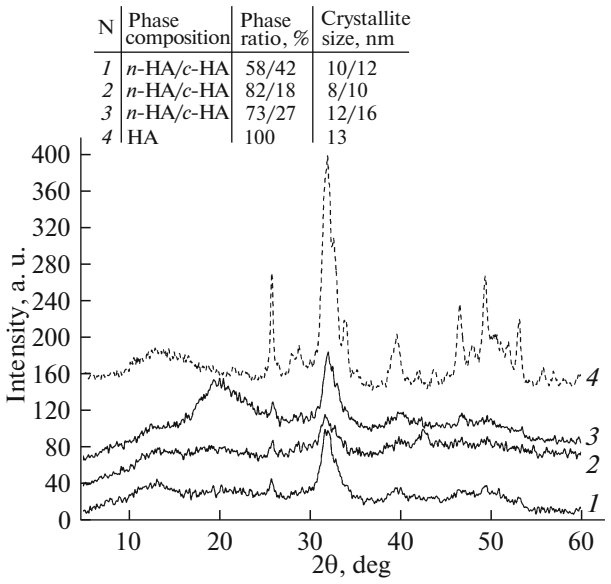

Fig. 1. Diffraction patterns of the bone matrix after 1 month: (*1*) normal, (*2*) with tuberculous osteitis, (*3*) with tuberculous osteitis after treatment, and (*4*) synthetic hydroxyapatite dried at 60°C; *n*-HA/*c*-HA = nonstoichiometric hydroxyapatite/carbonate hydroxyapatite.

received no specific treatment, while rabbits of group 3 underwent conventional antituberculosis therapy. Each group is composed of three individuals fed a conventional diet. Animals were removed from the experiment using lethal doses of Zoletil. Bone samples were cut from the primary focus and fixed in 2.5% glutaraldehyde prepared in a phosphate buffer solution. Then, the samples were cooled in liquid nitrogen, and serial chips were made in the same medium.

Synthetic amorphized hydroxyapatite (HA) $Ca_{10}(PO_4)_6(OH)_2$ powder [3–5], dried at 60°C to constant weight, which is as close as possible to the mineral component of bone tissue in structure and properties, was used as a reference sample.

The phase composition of the powdered bone matrix, dried to constant mass in air, was determined by X-ray phase analysis (XRD) using an ADVANCE D8 diffractometer (Bruker, Germany) with CuK_α = 1.5405 Å. IR spectroscopy was performed using a Tensor-27 spectrometer (Bruker, Germany) in the range of 400–4000 cm^{-1} (1 mg of bone powder per 800 mg KBr). Differential thermal analysis (DTA) was performed using a Netzsch STA 409 PC Luxx combined thermal analyzer (Germany) at a heating rate of 10.0°C/min in air (the sample weight was ~40 mg). Scanning electron microscopy (SEM) of bone slices was performed using an LEO 1420 microscope, combined with a Rontec elemental analysis unit (Germany). Gold was predeposited onto the surface of the samples.

RESULTS AND DISCUSSION

According to the X-ray diffraction data, it was found that the mineral component of healthy bone tissue is primarily represented by amorphized hydroxyapatite compared to synthetic hydroxyapatite (Fig. 1, diffraction patterns *1* and *4*). The mineral component of bone tissue is represented by 58% of nonstoichiometric hydroxyapatite and 42% of carbonate hydroxyapatite, which is consistent with the published data [6, 7]. In tuberculous osteitis, there is a significant decrease in the intensity of reflexes associated with the organic phase, against a significant increase in the amount of nonstoichiometric hydroxyapatite and a decrease in the size of crystallites of both nonstoichiometric hydroxyapatite and carbonate hydroxyapatite (Fig. 1, diffraction pattern *2*). In the diffraction pattern of the sample with tuberculous osteitis, there is a significant broadening of the X-ray amorphous halo, which indicates the maximum amorphization of hydroxyapatite. It can be assumed that in this case, the degree of amorphization is affected by the pathological processes [8] and, in particular, alkalosis characteristic of tuberculous intoxication. Under treatment conditions, the collagen skeleton of the bone matrix is restored; the epitaxial growth of hydroxyapatite crystallites takes place on the fibers of the bone matrix [2]. This is confirmed by X-ray diffraction data in the form of an X-ray amorphous halo at small angles 2θ of 16°–25° (Fig. 1, diffraction pattern *3*) and some increase in the degree crystallinity and hydroxyapatite crystallite size. Apparently, a weakly acidic medium, characteristic of regeneration, is formed in the regenerating bone matrix, which is confirmed by an increase in the amount of "acidic" carbonate hydroxyapatite.

The results of IR spectroscopy are consistent with the XRD data for bone powders, and the broadening of the bands on the IR spectra indicates a decrease in the crystallinity of calcium phosphates. In the IR spectra of bone powders of all groups of animals (Fig. 2, curves *1–3*), the stretching and deformation vibrations of the PO_4^{3-} tetrahedra at 1090, 1030, 970, 635, 613, and 560 cm^{-1} are broadened, which indicates distortion of the hydroxyapatite crystal lattice [9]. The presence of adsorbed water in the samples is confirmed by a broad absorption band at 3550–3200 cm^{-1} of stretching vibrations of water and a band at 1650 cm^{-1} of deformation vibrations of water. Structural OH groups, coordinated by the Ca^{2+} cation and not hydrogen-bonded in synthetic hydroxyapatite, are represented by a band at 3574 cm^{-1} (Fig. 2, curve *4*), while for bone powders, this band is shifted to 3744 cm^{-1} (Fig. 2, curves *1–3*). The presence of the organic phase is confirmed by the presence of bands at 3551, 3468, 3414, and 3204 cm^{-1} of stretching vibrations of the N–H and $-NH_2$ bonds, which overlap with stretching vibrations of the O–H bond; in the range of 2927–2855 cm^{-1}, of the C–H and $-CH_2-$ bonds; and

at 1745 cm^{-1}, of the C=O bonds [10]. The presence of a significant amount of the organic phase characteristic of group 3 of animals after treatment is confirmed by a sharp increase in the intensities of the C–H, $–CH_2–$, and C=O bonds (Fig. 2, curve *3*) with respect to the norm and in tuberculous osteitis.

The absorption bands of the C–O bond of carbonate ions at 1520, 1462, and 1412 cm^{-1} indicate the accumulation of CO_3^{2-} ions in the anionic hydroxyapatite sublattice [11, 12] and are confirmed by X-ray diffraction data on the presence of the carbonate hydroxyapatite phase. It can be assumed from the IR spectra that the presence of absorption bands at 1460, 1412, and 1520 cm^{-1} suggests substitution with carbonate ions, which can occur both in the A type (instead of OH^-) and B type (instead of PO_4^{3-}) [13, 14]. The preponderance of the B type anion substitution mechanism is typical for samples of groups 1 and 3, and in group 2 with tuberculosis osteitis, the A type of substitution dominates due to an increase in the intensity of the carbonate ion absorption band at 1520 cm^{-1} and a significant shift of the band of the OH group to 3744 cm^{-1}. We note that CO_3^{2-} substitutions have a deforming effect on the structure of hydroxyapatite because of the structural mismatch of the of CO_3^{2-} anions having a flat triangular shape replacing the PO_4^{3-} phosphate ions having the form of tetrahedra [9]. Therefore, stress sites may appear in substituted portions of the hydroxyapatite structure, and distortions appear in the lattice of the tetrahedral phosphate ion, resulting in the crystal becoming less stable. Because of carbonate substitutions, the concentration of hydroxyl groups decreases, the vibrational motions of atoms in the P–O bond become disordered, which disrupts the parallel packing of crystallites and, as a result, their epitaxial growth slows down. We can expect an increase in the chemical activity and resorbability of hydroxyapatite crystallites.

In addition, the intensity of the broad band in the range of 3414–3550 cm^{-1} (Fig. 2, curve *2*) increases for the bone matrix with tuberculous osteitis, which may indicate the appearance of "limestone" Ca–OH bonds in the hydroxyapatite structure. The mechanisms of these structural distortions are not clear, but it is undoubted that Mycobacterium tuberculosis have an affinity for potentially limestone hydroxyapatite centers, the formation of which is accompanied by an exothermic reaction and gives the crystallites and the bone matrix as a whole "binding" properties.

It was found by thermal analysis that the mass loss of the samples is observed in four temperature ranges (Fig. 3). In the first interval, at 70–200°C, there is a loss of adsorbed water, which is more pronounced for the sample of the control Group 1 (Fig. 3, curve *1*). Then, at 200–400°C, structural water and noncollagenous proteins are removed [14]. Moreover, under

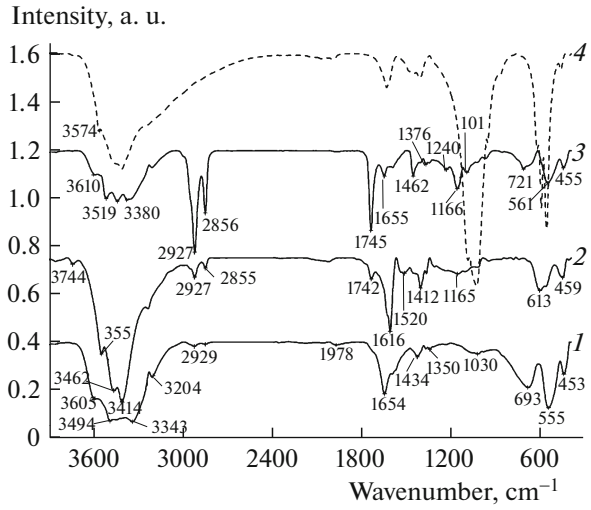

Fig. 2. IR spectra of the bone matrix after 1 month: (*1*) normal, (*2*) with tuberculous osteitis, (*3*) with tuberculous osteitis after treatment, and (*4*) synthetic hydroxyapatite dried at 60°C.

pathological conditions, dehydration occurs at lower energy values due to changes in the geometric parameters of ultrathin channels of the collagen matrix, which indicates their osteoporotic transformation (it was shown earlier in osteoporosis [2]). In the third interval, at 400–550°C, collagen is destroyed, and this stage is more pronounced for the sample of group 3 after treatment (Fig. 3, curve *3*), which contains the most substantial amount of the newly formed organic phase. At 550–900°C, carbon dioxide is removed from the mineral component of the bone matrix due to the transition of carbonate hydroxyapatite to stoichiometric hydroxyapatite [10, 11]. It should be noted that in the sample of bone matrix with tuberculous osteitis (Fig. 3, curve *2*), the third stage begins earlier, at 500°C, which may be due to the presence of a significant amount of amorphized calcium phosphate phases and the lowest concentration of the organic phase.

The presence of progressive tuberculous osteitis is verified by the observation of necrotic tissue and Mycobacterium tuberculosis of typical form adjacent to the primary focus of bone tissue in the bone matrix (Fig. 4). Morphologically, bacterial particles have the shape of semi-rounded cylinders; some of them form a structure of "full rings" (Fig. 4a). Moreover, normal Langhans cells, macrophages that have engulfed mycobacteria, are found in the depth of the matrix, 5 mm from the edge of the primary focus (Fig. 4b). These cells release multiple cytoplasmic processes, by which they are fixed to the free surfaces of the bone matrix. Perhaps this is because similar fixation of macrophages filled with mycobacteria is observed mainly in the lumens of microtubules or other pathologically free spaces (interstitial gaps, extended intercellular spaces in areas of osteoporosis). Thus, struc-

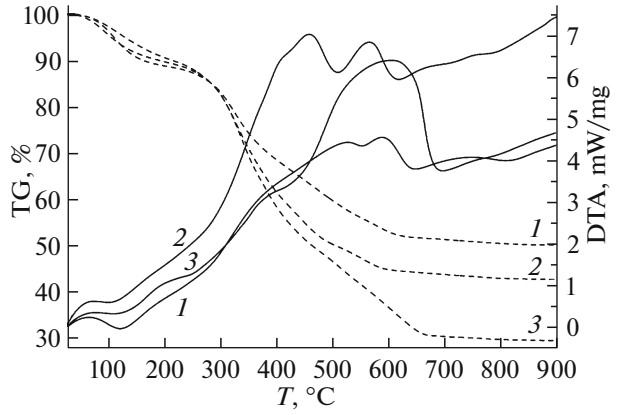

Fig. 3. Thermogravimetry (TG) and DTA curves of the bone matrix after 1 month: (*1*) normal, (*2*) with tuberculous osteitis, and (*3*) with tuberculous osteitis after treatment.

tural prerequisites are formed for sufficiently deep, up to 5–7 mm from the edge of the focus, penetration of macrophage carriers of mycobacteria.

Using SEM morphometry, we found that the volume ratio of regenerating bone tissue and dense fraction of the bone matrix varies in close proportions to the ratio of "acidic" and nonstoichiometric hydroxyapatite. Such a coincidence is not accidental and suggests that the "acidic" carbonate hydroxyapatite is accumulated mainly in regeneration foci, and the more "alkaline" nonstoichiometric hydroxyapatite accumulates in dense areas of the bone matrix. The enrichment with hydroxide groups "alkalizing" dense areas is indicated by an increase in the sizes of hydroxyapatite crystallites to 13 nm and an increase in the Ca-to-P (Ca/P) ratio to 3.06 (in the regeneration zone, Ca/P = 2.71), which shows the deposition of impurity calcium phosphate phases in tuberculosis osteitis.

According to the SEM data (Figs. 5a and 5b), a pronounced osteoporotic transformation with focal rarefaction and thinning of bone trabeculae is revealed in the bone matrix of animals of group 2 with tuberculous osteitis. Osteoporotic transformation is accompanied by fine disintegration and massive lysis of the bone matrix. After 2 months of development of the simulated tuberculous osteitis (Fig. 5b), fine disintegration of the bone matrix in the marginal regions of the bone adjacent to the focus reaches its maximum. It can be assumed that the osteoporotic transformation in the destruction zone creates prerequisites for the accumulation of filtrating forms of Mycobacterium tuberculosis and, in general, contributes to the emergence of drug-resistant bacilli.

Consequently, in tuberculous osteitis, the dense matrix looks like a "fracturing" at the micrometer level structureless interstitial fluid with multiple microcaverns. The dense matrix thickens the cortical plates, deforms the structure of the annular osteons, and increases the surface roughness of the interstitial osteons. Smooth cleavage osteons take the form of hyper-mineralized membranes with obliterated nanopores. At the same time, the micropores of the bone plates expand, which, due to the blockade of matrix nanopores, is aimed at compensating for the risks of deterioration of the transmembrane mass transfer. Borders of trabeculae scalloped by multiple microerosions, in a zone where no bone macrophages were found. Many erosions have a "thrombosed" appearance: they are filled with segregated particles of matrix detritus. Internal caverns are also filled with the same but swollen detritus, many of which communicate with each other and with the bone-marrow cavity through microcracks and fistulas. The above deformation structures indicate that in the morphogenesis of the destruction of a dense bone matrix, mechanochemical conflicts caused by the "alkaline" destruction of a "limestone" hydroxyapatite and accompanied by fragile disintegration of the matrix are of pri-

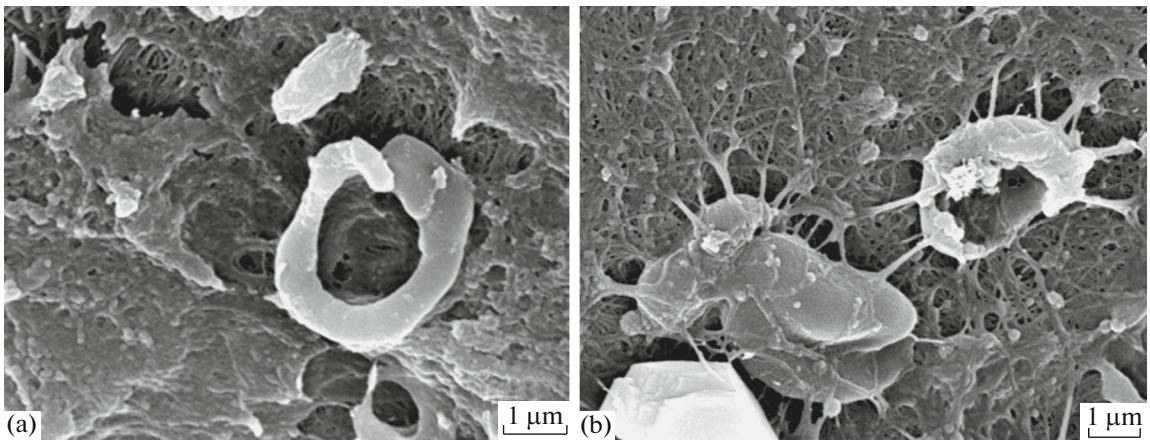

Fig. 4. SEM images of mycobacteria (a) oriented near the pore structures and (b) immobilized in Langhans cells.

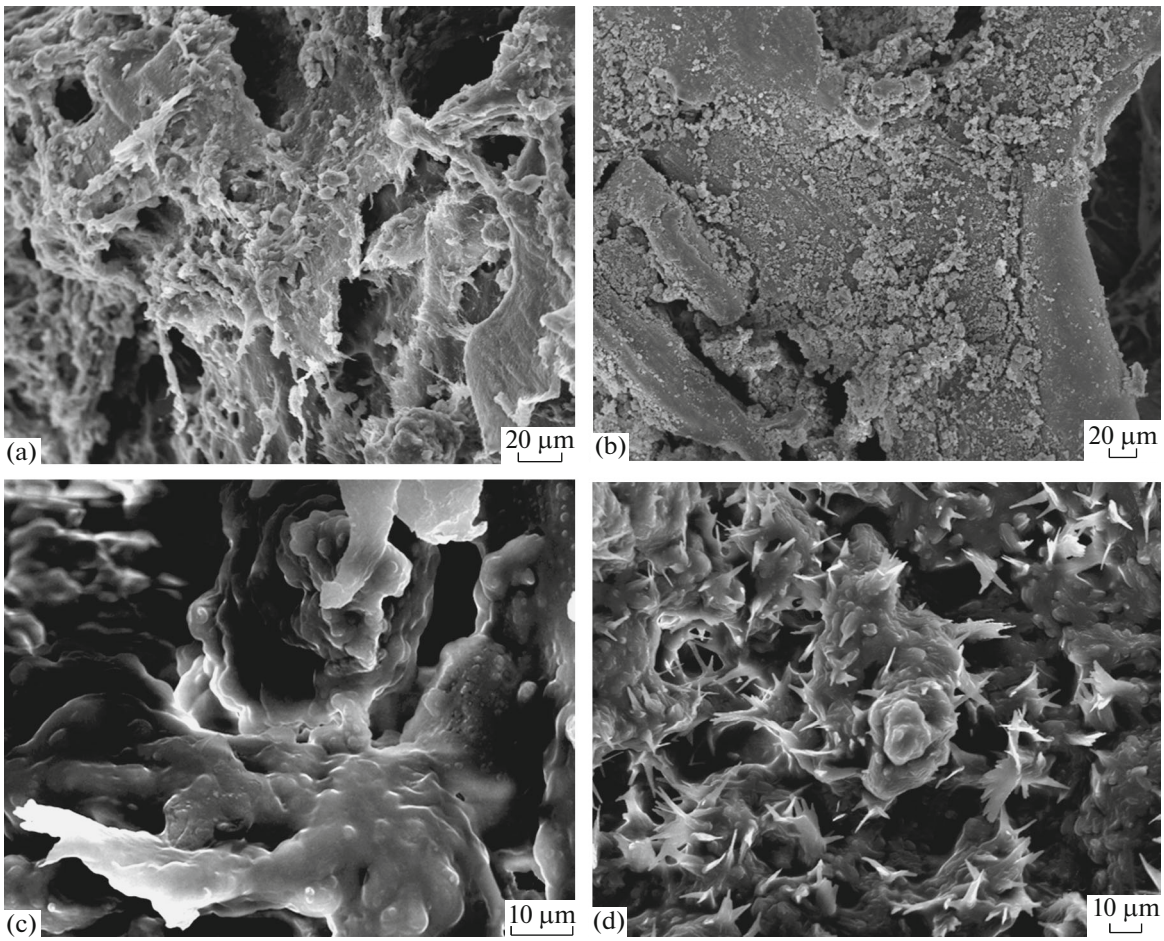

Fig. 5. SEM images of the bone matrix in tuberculous osteitis (a, b) without treatment and (c, d) after treatment: (a, c) 1 and (b, d) 2 months.

mary importance. The trend of such transformations is clear: the adsorption and destruction of bacterial particles in the "alkaline" debris of sequestered matrix fragments.

According to the SEM data (Figs. 5c and 5d), in animals of group 3, against the background of specific treatment of tuberculous osteitis, an increase in the number of foci of osteoblastic bone tissue remodeling is observed, indicating active regenerative processes. It is noteworthy that the number of such foci after 2 months of treatment increases significantly (Fig. 5d). In the foci of regeneration, hyperplasia of the matrix vesicles is recorded, osteoblasts with a typical process structure are accumulate, and polymorphic bone plates are formed. The processes of osteogenesis are unbalanced due to the uncontrolled growth of bone plates and trabeculae. The plates are oversaturated with calcium and grow into free volume in the form of lamellar-needle calcium phosphate phases, hydroxyapatite precursors such as octacalcium phosphate; many of them penetrate the intertrabecular space and the lumen of nascent Haversian channels.

CONCLUSIONS

Thus, the critical effects of the impact of Mycobacterium tuberculosis on the structure and physicochemical properties of the bone matrix are

1. A progressive and resistant to specific therapy increase in the amount of nonstoichiometric hydroxyapatite, accompanied by "alkalization" of the intercellular substance, precipitation of amorphized calcium phosphates, and embrittlement and fine disintegration of the bone matrix.

2. The predominance of the growth of carbonate hydroxyapatite crystals of mixed AB substitution type leads to an imbalance in the processes of remodeling and excessive osteogenesis, which is accompanied by the uncontrolled growth of bone trabeculae, mineral obliteration of micropores, and microphytization of the bone matrix.

3. The presence of limestone sites in the hydroxyapatite crystal lattice enhances the binding properties of the mineral phase of the bone matrix and promotes chemical immobilization and adhesion of Mycobacterium tuberculosis on their surface.

ACKNOWLEDGMENTS

This work was supported by the State Program of Scientific Research, Chemical Technologies and Materials (project no. 1.04).

REFERENCES

1. http://www.medvestnik.by/ru/sovremennii_podxod/-view/vnelegochnyj-tuberkulez-epidemiologicheskij-portret-6140-2008/.
2. A. A. Gaidash, L. N. Sinitsa, O. A. Babenko, and A. A. Lugovskoy, J. Osteoporos **2011**, 162041 (2011). doi 10.4061/2011/162041
3. V. K. Tsuber, L. A. Lesnikovich, A. I. Kulak, I. V. Trofimova, P. T. Petrov, T. V. Trukhacheva, Yu. D. Kovalenko, and V. L. Krasil'nikova, Khim.-Farm. Zh. **40** (8), 48 (2006).
4. V. K. Krut'ko, A. I. Kulak, and O. N. Musskaya, Inorg. Mater. **53**, 429 (2017). doi 10.1134/S0020168517040094
5. O. N. Musskaya, A. I. Kulak, V. K. Krut'ko, Yu. A. Lesnikovich, V. V. Kazbanov, and N. S. Zhitkova, Inorg. Mater. **54**, 117 (2018). doi 10.1134/S0020168518020115
6. R. M. Wilson, J. C. Elliot, and S. E. P. Dowker, Am. Mineral. **84**, 1406 (1999).
7. R. Z. Legeros, O. R. Trautz, J. P. Legeros, E. Klein, and W. P. Shirra, Science **155**, 1409 (1967).
8. O. A. Golovanova, S. A. Gerk, A. N. Kuriganova, and R. R. Izmailov, Sist. Metody. Tekhnol. **16** (4), 131 (2012).
9. A. M. Smolegovskii, *History of Phosphate Crystal Chemistry* (Nauka, Moscow, 1986).
10. R. A. Vlasov, E. P. Merkulova, V. F. Mel'nik, V. K. Krut'ko, A. I. Kulak, O. N. Musskaya, and N. V. Moskaleva, in *Proc. Sci.-Pract. Conf. "Topical Issues of Otorhinolaryngology," Blagoveshchensk, 2015*, p. 70.
11. J. P. Lafon, E. Championa, and D. Bernache-Assollant, J. Eur. Ceram. Soc. **28**, 139 (2008). doi 10.1016/j.jeurceramsoc.2007.06.009
12. V. S. Komlev, I. V. Fadeeva, A. N. Gurin, E. S. Kovaleva, V. V. Smirnov, N. A. Gurin, and S. M. Barinov, Inorg. Mater. **45**, 329 (2009).
13. S. A. Lemesheva, O. A. Golovanova, and S. V. Turenkov, Chem. Sustainable Dev. **17**, 319 (2009).
14. S. A. Lemesheva, O. A. Golovanova, I. V. Muromtsev, and S. V. Turenkov, Vestn. Omsk. Univ., No. 2, 106 (2010).

Translated by O. Zhukova